Nanofluid Convection in Microtubes

Joohyun Lee
e-mail: jhyunl@stanford.edu

Patricia E. Gharagozloo
e-mail: perahm@stanford.edu

Babajide Kolade

John K. Eaton

Kenneth E. Goodson

Department of Mechanical Engineering,
Stanford University,
Stanford, CA 94305

While there has been much previous research on the thermal conductivity and convection performance of nanofluids, these data are rarely reported together with effective viscosity data that govern the relevance for heat exchanger applications. We report here the effective convection coefficient and viscosity in microtubes ($D=0.5$ mm) along with stationary thermal conductivity measurements for nanofluids based on spherical particles (Al_2O_3, ZnO, and CuO) and carbon nanotubes. Sample data include an effective convection coefficient increase of 5% for 3 vol % Al_2O_3/DI water nanofluid, 13.3% for 4 vol % CuO/DI water nanofluid, and 11.6% for 0.2 vol % Carbon nanotube(CNT)/DI water nanofluid. When considered together with our viscosity measurement on the same fluids, we find that the only the CNT-based nanofluids are promising for microfluidic heat exchangers. [DOI: 10.1115/1.4001637]

Keywords: nanofluid, convection, heat transfer, carbon nanotubes, heat exchanger

1 Introduction

Fluid design considering thermal and viscous properties is a critical aspect of cooling system optimization for a variety of applications. This is particularly important for single-phase microfluidic heat exchangers for which the fluid thermal conductivity governs the thermal resistance and the viscosity governs the required pumping power at a given flowrate [1]. There is considerable interest in determining whether conventional heat transfer fluids, such as water, oils, and ethylene glycol, can be improved through nanoscale impurities. Recent data have suggested dramatic increases in the effective thermal conductivity of nanofluids with volume concentrations near or below 1% although the data have been inconsistent and incomplete from the perspective of fluid design. To make a rigorous determination of the potential relevance of nanofluids for heat exchangers, any increase in effective thermal conductivity must be weighed against the increase in effective viscosity.

Stationary nanofluid thermal conductivity data can be compared using an augmentation factor α_{cond}, which is defined using $k_{nano}/k_{bf}=1+\alpha_{cond}\phi$. In this equation, k_{nano} indicates the thermal conductivity of the nanofluid, k_{bf} is the conductivity of the base fluid, and ϕ is the nanoparticle volume concentration. Eastman et al. [2] reported a 60% thermal conductivity increase with 5 vol % of CuO/water nanofluid, yielding $\alpha_{cond}=12$. In a recent review, Kabelac and Kuhnke [3] reported that α_{cond} ranges from 2.5 to 6 for Al_2O_3/water and from 2.5 to 12 for CuO/water nanofluids. A significantly higher thermal conductivity increase was reported for Carbon nanotube(CNT)/water nanofluids. For example, Wen and Ding [4] measured $\alpha_{cond}=37$ and Zhang et al. [5] reported $\alpha_{cond}=50$ with CNT/water nanofluid. Regarding temperature dependence of nanofluid thermal conductivity, Chon et al. [6] reported that α_{cond} of Al_2O_3/water nanofluid varies from 2 to 7 at 20°C and at 70°C, respectively. Wen and Ding [4] observed α_{cond} of CNT/water nanofluid varies from 50 to 100 at 10°C and at 60°C, respectively. Most thermal conductivity data were obtained using the transient hot wire method, which measures the transient thermal response of a fine wire immersed in stationary fluids. In most cases, nanofluids were prepared by sonication of commercially available nanoparticles in a base fluid mixture. Frequently used particles included Al_2O_3, CuO, and CNT. The inconsistency of the past data indicates that many parameters can affect the thermal conductivity of nanofluids, such as particle size and shape, as well as the nanofluid preparation method and the fluid temperature.

Although there has been some research on nanofluid convection in macroscale tubes, these are rarely combined with measurements of pressure drop and effective viscosity. For consideration of convection applications, we define the convection heat transfer and viscosity augmentation factors α_{conv} and α_{visc} in an analogous manner to the thermal conductivity augmentation factor, as $h_{nano}/h_{bf}=1+\alpha_{conv}\phi$ and $\mu_{nano}/\mu_{bf}=1+\alpha_{visc}\phi$, respectively. Xuan and Li [7] measured 60% heat transfer coefficient increase with 2 vol % Cu/water nanofluid, which corresponds to $\alpha_{conv}=30$ under turbulent flow condition in a 10 mm diameter tube. They reported no change in the pressure drop with the addition of nanoparticles ($\alpha_{visc}=0$). Ding and co-workers [8,9] measured a substantial heat transfer improvement with Al_2O_3/water($\alpha_{conv}=30$) and CNT/water($\alpha_{conv}=350$) nanofluids under laminar flow conditions in a 4.5 mm diameter tube. Pressure drop data were not reported for their experiments. Lee and Mudawar [10] did not observe a large heat transfer increase ($\alpha_{conv}=3$) in a 341 μm hydraulic diameter microchannel with Al_2O_3/water nanofluid. They found that the pressure drop increased much more than expected from effective medium models. Rea et al. [11] and Williams et al. [12] investigated the convective heat transfer of Al_2O_3/water and Zirconia/water nanofluids in laminar and turbulent conditions, respectively. The results showed that the heat transfer coefficients and pressure drop of nanofluids can be accurately predicted by the traditional models. Because there are so few data available for the convective heat transfer and pressure drop of nanofluids, their usefulness as a heat transfer liquid in microchannels is still open to debate.

The present work measures the effective thermal conductivities in a laminar convection situation and viscosities of nanofluids containing CNTs as well as spherical oxide nanoparticles in a 500 μm microtube in laminar flow. The data are compared with stationary thermal conductivity data, also measured here for the same fluids. Nanofluids are prepared by using intensive sonication of the nanoparticles and base fluid mixture. To characterize nanofluids, we measured the nanoparticle size in nanofluids using a dynamic light scattering (DLS) system. Furthermore, SEM images were taken to investigate the morphology of nanoparticles.

Contributed by the Heat Transfer Division of ASME for publication in the JOURNAL OF HEAT TRANSFER. Manuscript received December 12, 2009; final manuscript received March 16, 2010; published online July 7, 2010. Assoc. Editor: Robert D. Tzou.

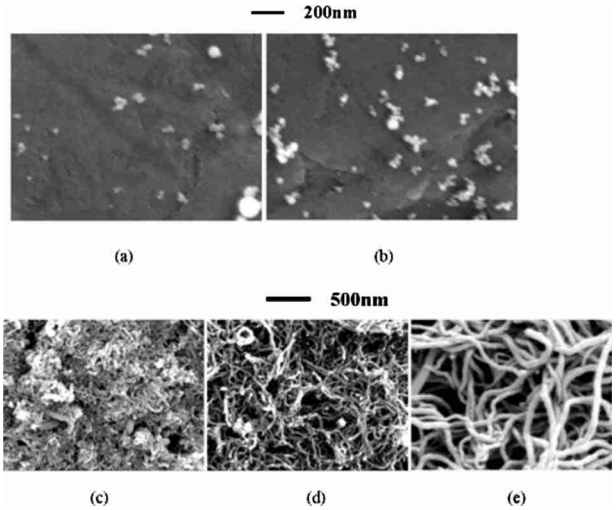

Fig. 1 Scanning electron microscopy images of (*a*) Al_2O_3 nanoparticles(40–50 nm), (*b*) CuO nanoparticles(13–37 nm), (*c*) multiwall CNT(A) (10–30 nm and 1–10 μm), (*d*) multiwall CNT(B) (10–30 nm and 0.5–50 μm), and (*e*) multiwall CNT(C) (40–60 nm and 5–15 μm) after evaporation of deionized water in nanofluids

2 Nanofluid Preparation and Preliminary Characterization

Nanofluids were prepared by applying a strong 1 h sonication using an ultrasonic probe (Hielscher Ultrasonics, Teltow, Germany) of commercially available nanoparticles and deionized water mixture. The Al_2O_3, CuO, and ZnO nanoparticles were purchased from Alfa Aesar Corp., Ward Hill, MA, and multiwall Carbon nanotubes (A), (B), and premade Al_2O_3 nanofluids were purchased from Sigma–Aldrich, St. Louis, MO. Multiwall CNT(C) was purchased from SES Research, Houston, TX. In the case of CNT/DI water nanofluids, gum arabic was added as a surfactant to produce a stable suspension. The prepared oxide nanofluids were stable for approximately 6 h and some sedimentation was observed after that period. The average particle size of spherical nanoparticles was measured by a particle size analyzer (90Plus, BIC Corp., Holtsville, NY). This equipment is based on the principle of DLS. The measured particle size was 155 nm for Al_2O_3/DI water nanofluids, 326 nm for CuO/DI water nanofluids, 371 nm for ZnO/DI water nanofluid, and 90 nm for premade Al_2O_3/DI water nanofluids. The measured particle size was at least four times larger than the nominal particle size claimed by the vendor. This finding implies that there are numerous agglomerated nanoparticles in the prepared nanofluids. Several efforts such as pH variation and a longer sonication time were attempted to separate the agglomerated nanoparticles in hopes of obtaining higher thermal conductivity increase. However, an effective particle size reduction method was not found. Figure 1 shows SEM images of the Al_2O_3, CuO nanoparticles, and three different kinds of multiwall CNT. For the sample preparation, several droplets of nanofluids were placed on the sample holder by pipette and dried in air. After the nanofluids were completely dried, a thin gold layer was applied using a sputter coater.

The SEM images showed that numerous particles were agglomerated for Al_2O_3 and CuO nanoparticles as expected. The agglomerated size was approximately equal to the DLS result. The SEM images of the three CNT samples show very different CNT shapes. The CNT(A) was composed of some short, irregular carbon tubes and many amorphous carbon pieces. On the other hand, the CNT(B) and CNT(C) had relatively long, uniform tube shape.

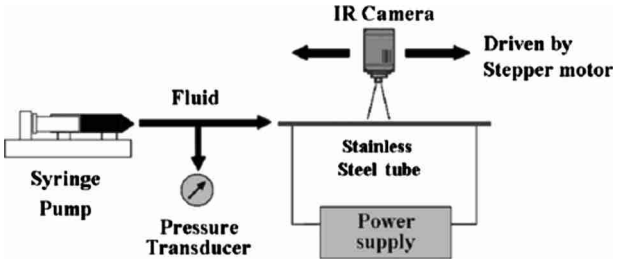

Fig. 2 Experimental apparatus of convection and pressure drop measurement. infrared camera measures the outside wall temperature of stainless steel tube heated by power supply; pressure transducer measures the pressure drop in the microtube

3 Thermal Convection Experiments in Microtubes

A simple microtube experiment was developed to measure the convection performance of nanofluids. Figure 2 illustrates the experimental apparatus. A 10 cm long stainless steel tube (Goodfellow Corp., Oakdale, PA) with an inside diameter of 500 μm was used as the test section. A syringe pump delivered fluid into the microtube at a constant flowrate. The test section was heated by passing dc power along the tube length. A constant heat flux condition was achieved along the tube due to the low thermal conductivity (16.3 W/m K) of stainless steel. A midwavelength (3–5 μm) infrared (IR) camera (Indigo Systems Corp., Goleta, CA) was mounted on a stepper motor driven traverse, which allowed the IR camera to move along the whole test section. A pressure transducer was connected near the inlet of the microtube to measure the pressure drop.

The calibration of the IR camera was conducted by using an electrically heated copper block heat exchanger. The microtube was connected to the outlet of the heat exchanger. Water was pumped into the heat exchanger through the microtube at a high flowrate. The calibration curves were obtained by measuring the copper block temperature with a K-type thermocouple and correlating the temperature with the intensity of the tube image taken by the IR camera.

Figure 3 shows the wall temperature data for DI water, 0.1 vol % and 0.2 vol % concentration CNT(B)/DI water nanofluids. The flowrate was 7 ml/min, the corresponding Reynolds number was 330, and 10 W power was applied to the test section. At the downstream region, the wall temperature decreased mono-

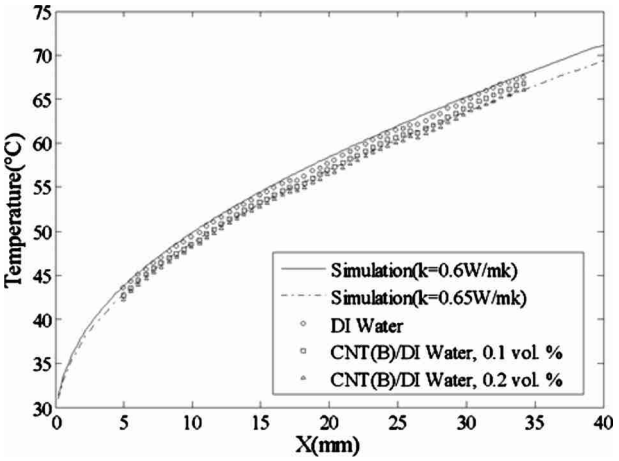

Fig. 3 Wall temperature distributions of DI water, 0.1 vol % and 0.2 vol % CNT(B)/DI water nanofluid data; effective thermal conductivity is extracted by performing conjugate simulation

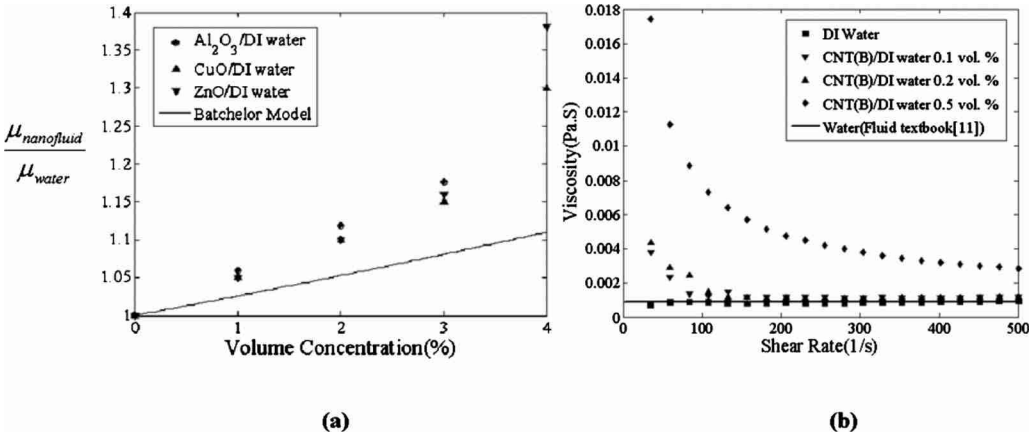

Fig. 4 (*a*) **Effective viscosity data of Al_2O_3/DI water, CuO/DI water, and ZnO/DI water nanofluids. Viscosity data were obtained by measuring the pressure drop in the microtube. Batchelor model of particle laden flow fail to predict the nanofluid viscosity.** (*b*) **Viscosity variation in CNT(B)/DI water nanofluids as a function of shear rate showing non-Newtonian shear-thinning behavior. Viscosity was measured using a rheometer.**

tonically with the increasing particle volume concentration, which indicates the effective thermal conductivity increase in the nanofluids. In order to estimate the thermal conductivity increase, a conjugate simulation was conducted. In the simulation, a constant thermal conductivity was used so the simulation did not consider the temperature-dependent thermal conductivity. A heat loss from the tube surface to the ambient air due to the natural convection was considered in the simulation based on the correlation provided by Churchill and Chu [13]. The calculated value of the nanofluid thermal conductivity was relatively insensitive to the natural convection heat transfer coefficient used in the analysis. For example, a doubling of the heat transfer coefficient resulted in only a 3% change in the calculated thermal conductivity. Validation of this experiment was achieved by confirming that results for plain water matched the simulation result within 1 °C. After the simulation was matched with the water data, the thermal conductivity of the fluid in the simulation was increased until the tube wall temperature in the simulation matched the nanofluid temperature data. The value of the conductivity, which produced the best fit to the temperature data, was taken as the effective thermal conductivity of the nanofluid. The possible sources of measurement uncertainty were IR camera noise and calibration uncertainty, electrical power measurements of the applied heat flux, estimates of the convective losses, and thermocouple uncertainty. The biggest contribution to the uncertainty in the effective thermal conductivity was the IR camera, which contributed 2.1% uncertainty. The total uncertainty in the effective thermal conductivity measurements was less than 5.2%. This estimate was confirmed by repeated measurements of plain water, which always fell within 4% of the known value. One concern was that a given nanofluid could leave a residue on the tube surface, which would affect subsequent measurements. The tube was thoroughly rinsed with DI water between nanofluid measurements and the water measurements were repeated to confirm that there was no remaining effect of the nanofluid.

The effective thermal conductivity was increased by 8.3% for 0.2% volume concentration CNT(B)/DI water nanofluids. The corresponding α_{conv} value was 41.5. CNT nanofluids with higher concentration could not be measured due to the tube clogging problem. The CNT nanofluid at 0.3 vol % could not be pumped through the microtube by the syringe pump. The same procedures were carried out for the oxide nanofluids with concentrations ranging from 1 vol % to 4 vol %.

It is important to note that our analysis relating the tube wall temperature distribution to fluid conductivity assumes that the conductivity of the nanofluid is uniform. It is possible that the nanofluid particles could produce a nonuniform conductivity in the tube. In any case, the present measurements yield an effective conductivity value, which is what would be needed for the analysis of a convective heat transfer system.

The viscosity data for nanofluids were obtained by measuring the pressure drop in the microtube. The hydrodynamic entrance length was 7.5 mm when the Re number was 300. When fully developed, the laminar flow is assumed along the entire tube, a circular Poiseuille flow is achieved and the viscosity of fluid is directly proportional to the pressure drop in the tube. The circular Poiseuille flow is given in the following equation:

$$Q = -\frac{\pi d^4}{128\mu}\frac{dp}{dx} \tag{1}$$

In this equation, Q is a flowrate and d is an inner diameter of the tube. Therefore, the effective viscosity of the fluid could be determined by measuring the pressure drop through the microtube.

The uncertainty of the effective viscosity measurement was estimated to be less than 5% considering the uncertainty of the flowrate from the syringe pump and the pressure measurement uncertainty [14]. The experiment was validated by confirming that the measured viscosity of DI water matched tabulated values. The pressure drop with pure water was measured after each nanofluid measurement to ensure that the tube had not been partially clogged by nanoparticles. Figure 4(*a*) shows viscosities of the oxide nanofluids compared with water viscosity as a function of the particle volume concentration. The viscosity of nanofluids was increased significantly as a strong function of the particle volume concentration. The traditional Batchelor model of particle laden fluid [15] underpredicts the increase in the viscosity of nanofluids. The agglomerated nanoparticles appeared to increase the viscosity more rapidly than predicted by the Batchelor model. The Batchelor model explains the effective viscosity of a spherical particle laden fluid by considering the effect of hydrodynamic interaction of pairs of spheres and Brownian motion. The equation is shown below.

$$\mu^* = \mu(1 + 2.5\phi + 6.2\phi^2) \tag{2}$$

Here, μ^* is the effective viscosity, μ is the base fluid viscosity, and ϕ is the volume concentration of particles.

The viscosity of CNT(B)/DI water nanofluid was also measured by a rheometer (AR2000, TA Instruments, New Castle, DE). Figure 4(*b*) presents the viscosity variation in the CNT(B)/DI water nanofluid as a function of shear rate. The viscosity decreased ex-

Table 1 Measured thermal conductivities and viscosities of various nanofluids: all data are taken from microtube experiment

	Volume concentration (%)	k_{eff} (W/m K)	μ_{eff} ((Pa s)$\times 10^{-3}$)
Al_2O_3/DI water	3	0.63	7.13
Premade Al_2O_3/DI water	8	0.7	1.05
CuO/DI water	4	0.68	1.23
ZnO/DI water	4	0	1.16
CNT(A)/DI water	0.2	0	1.16
CNT(B)/DI water	0.2	0.65	1.09
CNT(C)/DI water	0.2	0.67	1.16

ponentially as the shear rate was increased over the entire shear rate of 0–500 (1/s). Thus the CNT(B)/DI water nanofluid has non-Newtonian shear-thinning behavior.

All the thermal conductivity and viscosity data obtained from microtube experiment are summarized in Table 1 at the maximum volume concentration.

4 Stationary Thermal Conductivity Measurements

The thermal conductivity of stationary nanofluids was also measured by the apparatus shown in Fig. 5 [16]. One inch square, copper plates spaced 500 μm apart hold the nanofluid. This spacing yields an average Rayleigh number of less than 10^3 and scaling analysis confirms that bulk fluidic motion due to buoyancy forces is negligible. A 250 μm thick Kapton heater (Omega/KHLV-101) generates Joule heat, which conducts across the nanofluid, and dissipates into a Peltier cooler and heat sink. A heat flux sensor (Omega/HFS-3) monitors the heat flux. The temperature distribution is measured with a high-resolution infrared microscope (QFI/Infrascope). The IR focal plane array is 256×256 InSb with 2–5.5 μm wavelength detection and 0.1 K temperature sensitivity. A 15×, 1.0 numerical aperture, Si/Ge objective obtains a 2.8 μm resolution. The 256 temperature lines are ensemble averaged. An encasing humidification chamber reduces evaporation.

A 20 μm thick polyester film covers the fluidic opening, serves as a uniform emissivity emitter, counteracts averaging effects from the IR penetration in water, and reduces fluid evaporation. The heat flux traveling through the film is calculated using a thermal resistor network as less than 0.06% of the applied heat flux. A COMSOL finite element thermal model predicts the difference in the calculated thermal conductivity from the temperature of the film compared with the fluid temperature of less than 1%. The emissivity is calibrated for each measurement with a two temperature surface emissivity correction at characteristic temperatures. The calibration is applied to the measurement images and corrects for reflected signal components and emissivity spatial and temperature dependencies.

Heat loss from the apparatus to the environment is due to natural convection from the outer surfaces, conduction through the back insulator, and fluid evaporation. These losses are found to be less than 5% of the applied heating power and are systematically eliminated as part of the data extraction procedure. The ability to precisely determine the temperature-dependent conductivity of pure water is verified before each measurement. The thermal conductivities have repeatability to within 5% of the average value.

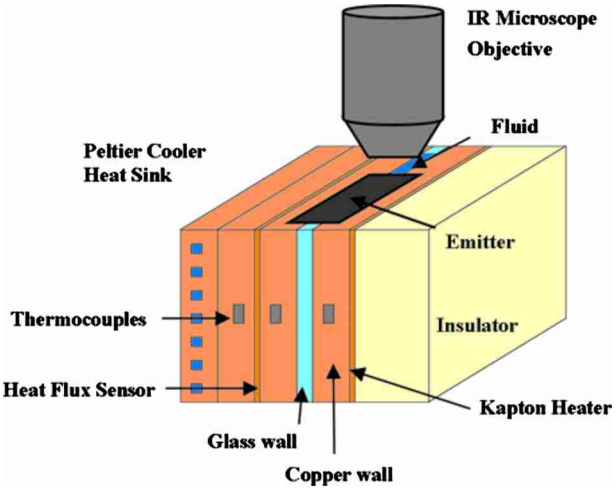

Fig. 5 Schematic of experimental apparatus measuring thermal conductivity of stationary nanofluids

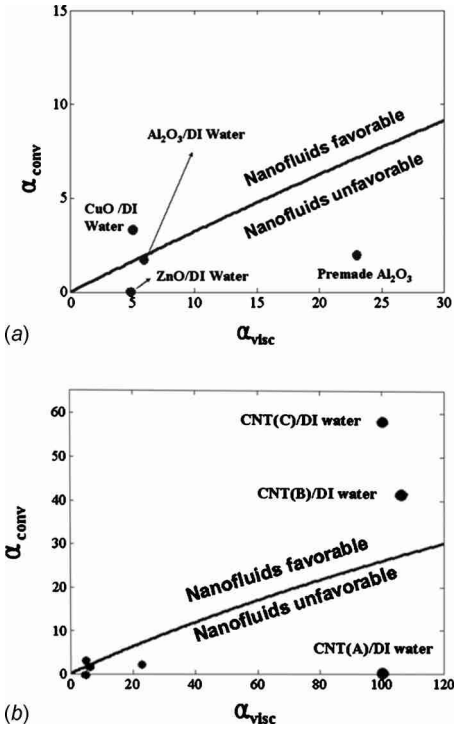

Fig. 6 Effective viscosity and heat transfer augmentation data of seven different nanofluids: CNT(A)/DI water, CNT(B)/DI water, CNT(C)/DI water, CuO/DI water, Al_2O_3/DI water, ZnO/DI water, and premade Al_2O_3/DI water; all data are obtained from microtube experiment

5 Results and Discussion

Figure 6 shows the α_{conv} and α_{visc} data of seven different nanofluids. These data are obtained from only the microtube experiment. A boundary line, which determines the effectiveness of nanofluids, is drawn in the same figure. This boundary line was

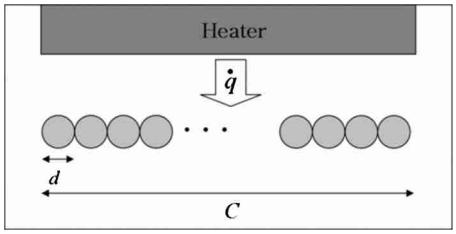

Fig. 7 Multiple parallel channels with each diameter of *d*; the total channel width is constant as *C*

Table 2 Effective heat transfer augmentation data of four nanofluids: CNT(B)/DI water, CNT(B)/silicone oil, Al_2O_3/DI water, and premade Al_2O_3/DI water: data are obtained from microtube experiment, stationary experiment, and macrotube experiment

	α_{conv} from microtube	α_{cond} from stationary [16,17]	α_{conv} from macrotube [18]
CNT(B)/DI water	41.5	40	Not measured
CNT(B)/silicone oil	Not measured	42	43
Al_2O_3/DI water	1.7	8	4
Premade Al_2O_3/DI water	2	3	Not measured

calculated by analyzing the flow and heat transfer of a coolant passing through parallel channels in a heated chip.

A schematic of a multiple parallel channel cooling system is shown in Fig. 7. A total heat transfer rate of $\dot{q}$ is uniformly distributed into each channel with a diameter d. The total width of the channels is fixed as a constant C. The total number of channels and the channel diameter can vary. We also assume hydrodynamically and thermally fully developed flow and all the fluid properties other than thermal conductivity and the viscosity stay the same. The constraints are the fixed total flowrate and the fixed pumping power. Other constraints could be chosen but the present choice would be typical for a designer deciding on the use of a nanofluid in a given cooling system.

Under these conditions, we find the minimum thermal conductivity increase needed to offset the decrease in flowrate caused by the viscosity increase in nanofluids. The result shows that nanofluid is effective as long as the thermal conductivity increase in the nanofluid is higher than the one third power of the viscosity increase.

From the results of Fig. 6, all the oxide nanofluids are not useful except CuO/DI water nanofluid. On the other hand, the CNT(B) and CNT(C)/DI water nanofluids are more effective than DI water despite the high α_{visc} value. CNT(A)/DI water should not be used. The remarkable point is the high α_{conv} values of CNT nanofluids. The CNT shape from the SEM images in Fig. 1 appears to affect the increase in the thermal conductivity. The CNT(B) and CNT(C) samples had long uniform tube shape and gave the result of extremely high α_{conv} of 41.5 and 58, respectively. The CNT(A) had short irregular tube shape and showed zero α_{conv} value. Although it is important to note that despite the large α_{conv} value for CNT nanofluids, the maximum increase in thermal conductivity was only 11.6%.

The effective thermal conductivity data obtained from the stationary experiment [16,17] and a 5 mm diameter macrotube convection experiment [18] are tabulated in Table 2 along with the results of the microtube experiment. The stationary measurement confirms the increase in the high thermal conductivity of CNT(B)/DI water nanofluids.

6 Summary and Concluding Remarks

In this work, several nanofluids are prepared and characterized by measuring the particle size using DLS system and by taking SEM images. The effective thermal conductivity of nanofluids is measured by microtube convection experiments and stationary thermal conductivity measurement. Viscosity data were acquired by measuring the pressure drop for laminar tube flow and using a rheometer. The effectiveness of a nanofluid for electronic cooling application is calculated by its thermal conductivity and viscosity.

When we compared the experimental data and the nanofluid effectiveness line, the results show oxide nanofluids are not effective so they should not be used in applications. Certain CNT nanofluids are effective despite the high viscosity increase.

The thermal conductivity of the CNT nanofluids is closely related to the shape of the nanotubes because only the long and uniform tubes increase nanofluid thermal conductivity significantly. However, CNT nanofluids can cause a clogging problem as well as an abrasion problem in the microchannel heat exchanger because numerous CNTs in the nanofluids are entangled and adhere to each other forming large clusters.

Acknowledgment

The authors gratefully acknowledge the financial support of the Office of Naval Research overseen by Dr. Mark S. Spector under Grant No. N00014-05-1-0374-P00001.

References

[1] Prasher, R. P., Song, D., Wang, J., and Phelan, P., 2006, "Measurements of Nanofluid Viscosity and Its Implications for Thermal Applications," Appl. Phys. Lett., **89**, p. 133108.
[2] Eastman, J. A., Choi, U. S., Li, S., Thompson, L. J., and Lee, S., 1996, "Enhanced Thermal Conductivity Through the Development of Nanofluids," *Proceedings of Materials Research Society Symposium*, Boston, MA, Dec. 2–5, Vol. 457, pp. 3–11.
[3] Kabelac, S., and Kuhnke, J. F., 2006, "Heat Transfer Mechanisms in Nanofluids—Experiments and Theory," Annals of the Assembly for International Heat Transfer Conference 13.
[4] Wen, D., and Ding, Y., 2004, "Effective Thermal Conductivity of Aqueous Suspensions of Carbon Nanotubes(Carbon Nanotube Nanofluids)," J. Thermophys. Heat Transfer, **18**(4), pp. 481–485.
[5] Zhang, X., Gu, H., and Fujii, M., 2006, "Effective Thermal Conductivity and Thermal Diffusivity of Nanofluids Containing Spherical and Cylindrical Nanoparticles," J. Appl. Phys., **100**, p. 044325.
[6] Chon, C., Kihm, K., Lee, S., and Choi, S., 2005, "Empirical Correlation Finding the Role of Temperature and Particle Size for Nanofluid (Al_2O_3) Thermal Conductivity Enhancement," Appl. Phys. Lett., **87**, p. 153107.
[7] Xuan, Y., and Li, Q., 2003, "Investigation on Convective Heat Transfer and Flow Features of Nanofluids," ASME J. Heat Transfer, **125**, pp. 151–155.
[8] Wen, D., and Ding, Y., 2004, "Experimental Investigation Into Convective Heat Transfer of Nanofluids at the Entrance Region Under Laminar Flow Conditions," Int. J. Heat Mass Transfer, **47**, pp. 5181–5188.
[9] Ding, Y., Alias, H., Wen, D., and Williams, R. A., 2006, "Heat Transfer of Aqueous Suspensions of Carbon Nanotubes," Int. J. Heat Mass Transfer, **49**, pp. 240–250.
[10] Lee, J., and Mudawar, I., 2007, "Assessment of the Effectiveness of Nanofluids for Single-Phase and Two-Phase Heat Transfer in Micro-Channels," Int. J. Heat Mass Transfer, **50**, pp. 452–463.
[11] Rea, U., McKrell, T., Hu, L., and Buongiorno, J., 2009, "Laminar Convective Heat Transfer and Viscous Pressure Loss of Alumina-Water and Zirconia-Water Nanofluids," Int. J. Heat Mass Transfer, **52**, pp. 2042–2048.
[12] Williams, W., Buongiorno, J., and Hu, L., 2008, "Experimental Investigation of Turbulent Convective Heat Transfer and Pressure Loss of Alumina/Water and Zirconia/Water Nanoparticle Colloids (Nanofluids) in Horizontal Tubes," ASME J. Heat Transfer, **130**, p. 042412.
[13] Churchill, S. W., and Chu, H. H. S., 1975, "Correlating Equations for Laminar and Turbulent Free Convection From a Horizontal Cylinder," Int. J. Heat Mass Transfer, **18**, pp. 1049–1053.
[14] White, F. M., 1991, *Viscous Fluid Flow*, 2nd ed., McGraw-Hill, New York.
[15] Batchelor, G. K., 1977, "The Effect of Brownian Motion on the Bulk Stress in a Suspension of Spherical Particles," J. Fluid Mech., **83**, pp. 97–117.
[16] Gharagozloo, P. E., Eaton, J. K., and Goodson, K. E., 2008, "Diffusion, Aggregation, and the Thermal Conductivity of Nanofluids," Appl. Phys. Lett., **93**, p. 103110.
[17] Gharagozloo, P. E., Eaton, J. K., and Goodson, K. E., 2007, "Impact of Thermodiffusion on Temperature Fields in Stationary Nanofluids," *Proceedings of ASME Interpack*, Vancouver, BC, Canada, Jul. 8–12.
[18] Kolade, B., Goodson, K. E., and Eaton, J. K., 2009, "Convective Performance of Nanofluids in a Laminar Thermally Developing Tube Flow," ASME J. Heat Transfer, **131**(5), p. 052402.